# Grafting of Molecularly Imprinted Polymer Films on Silica Supports Containing Surface-Bound Free Radical Initiators

**Claudia Sulitzky, Bärbel Rückert, Andrew J. Hall, Francesca Lanza, Klaus Unger, and Börje Sellergren***

*Department of Inorganic Chemistry and Analytical Chemistry, Johannes Gutenberg Universität Mainz, Duesbergweg 10-14, 55099 Mainz, Germany*

*Received July 23, 2001; Revised Manuscript Received October 5, 2001*

ABSTRACT: Silica particles containing surface-bound free radical initiators have been used as supports for the grafting of thin films of molecularly imprinted polymers (MIPs). This technique offers a means of fine-tuning the layer thickness for improved kinetic properties or enhanced capacity in chromatographic or sensor applications. Thus prepared MIPs imprinted with L-phenylalanine anilide, have been characterized by FT-IR spectroscopy, thermogravimetric analysis (TGA), differential scanning calorimetry (DSC), elemental analysis, fluorescence microscopy, and scanning electron microscopy (SEM), providing evidence concerning the reproducibility in each step and the quantity and quality of the grafted films. The chromatographic properties of the materials have been investigated with respect to the average layer thickness of the polymer on the surface, the solvent, the support pore diameter, the cross-linker concentration, and the composition of the mobile phase. For the porous particles, the column efficiency depended strongly on the amount of grafted polymer. Thus, polymers grafted as thin films (ca. 0.8 nm as average film thickness) on silica with 10 nm average pore diameter showed the highest column efficiency giving plate numbers ($N$) for the imprinted enantiomer of ca. 700 $m^{-1}$ and for the antipode ca. 24 000 $m^{-1}$. This resulted in baseline resolutions on a 33 mm long column in less than 5min. On the other hand the sample load capacity and separation factor increased up to 7.0 nm layer thickness and dropped again for larger amounts of grafted polymer. A support with an average pore diameter of 100 nm and a 3.8 nm layer thickness showed a far higher saturation capacity than values previously determined for the conventional monolithic materials.

## Introduction

Molecular imprinting has become an established technique to prepare robust molecular recognition elements toward a wide variety of target molecules.[1−4] The relative ease of preparing the molecularly imprinted polymers (MIPs) has led to their assessment as substitutes for antibodies or enzymes in chemical sensors, catalysis and separations. Presently used techniques to prepare MIPs most often result in materials exhibiting high affinity and selectivity but low capacity and poor site accessibility for the target molecule or molecules.[5−7] This leads to long response times when the materials are assessed as recognition elements in chemical sensors and broad, asymmetric peaks when they are assessed as stationary phases in the chromatographic mode. The MIPs are obtained as monoliths and useful particles can only be obtained after crushing and sieving cycles, leading to a large loss of material. As a consequence, these materials are assessed mainly as molecular recognition elements for analytical quantifications, e.g. chemical sensors[8] or solid-phase extraction,[9] and thus are in formats which are not dependent on high sample load capacity, chromatographic efficiency, or large quantities of material.

To advance into preparative scale applications or high efficiency separations, new MIP morphologies and manufacturing techniques need to be developed. A robust manufacturing technique should result in a high yield of uniform particles, with particle and pore size distributions controlled independently of the monomers, templates and solvents used in the synthesis of the MIP.

MIPs in the bead format have previously been prepared through suspension polymerization techniques,[10−13] core−shell emulsion polymerization[14] or dispersion/precipitation polymerization techniques.[15−17] This has resulted, in some cases, in spherical particles of a narrow size distribution with improved recognition or kinetic properties. Unfortunately, the conditions needed to generate sites of high affinity are often incompatible with the conditions needed to obtain the desired particle morphologies. Therefore tedious trial and error is often needed to arrive at an acceptable compromise. These problems can be overcome by grafting techniques where the MIPs are grown on preformed support materials of known morphology.[18−22] For instance, MIPs have been prepared as grafted coatings on silica supports,[18,20] on organic polymer supports[19−22] and on the walls of fused silica capillaries.[23−25] Most of these coatings have been prepared by grafting polymers to the various surfaces. Thus, prior to polymerization, the surface contains polymerizable double bonds that can add to the growing polymer chains in solution, thus linking them to the surface. One problem with this technique is the presence of initiator in solution, requiring the monomer mixture to be applied as a liquid thin film on the surface prior to polymerization. Thus, the exact amount of monomers that will coat the available surface with a liquid film up to ca. 10 nm thick is dissolved together with initiator in an excess of solvent. Thereafter, the modified support is added and the solvent evaporated to leave the monomer film and initiator on the surface. Polymerization is then usually carried out at elevated temperatures. With this procedure, the thickness of the polymer layer is difficult to control and capillary forces upon evaporation of solvent may cause incomplete wetting of the surface. Moreover, the maximum density of grafted polymer chains is here limited due to kinetic and steric factors.

10.1021/ma011303w CCC: $22.00 
Published on Web 12/07/2001

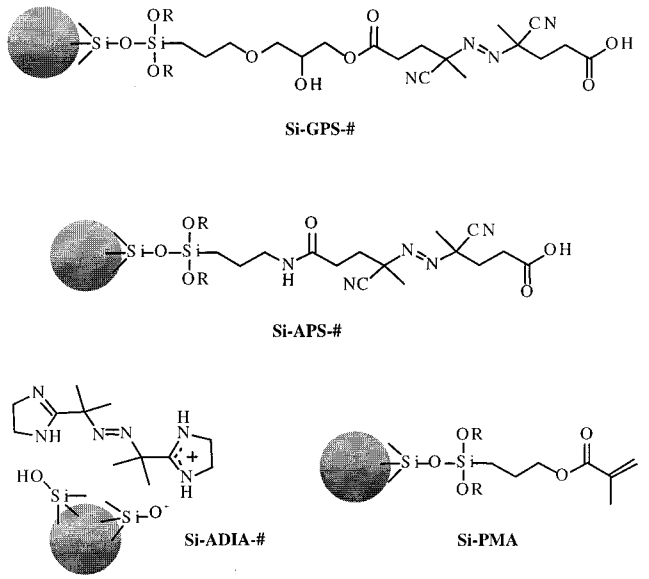


**Figure 1.** Surface modifications used in the study. The silica supports were modified covalently in two steps with GPS or APS and the azoinitiator ACPA (Si-GPS-# or Si-APS-#) or noncovalently in one step with the diamidine azoinitiator ADIA. Si-PMA was used in the "grafting to" experiments.

By confining the initiating radicals to the support surface (Figure 1),[26,27] a higher density of grafted polymer chains can be achieved.[28,29] In the absence of chain transfer, this would lead to chain growth occurring mainly from the surface of the support with minimal polymerization occurring in solution. In the preparation of MIP coatings, this would have interesting consequences. For instance, the polymerization could be carried out at the surface of initiator-modified support particles suspended in a mixture of the monomers and solvent. This would allow polymerization in a simple tank reactor by either thermal or photochemical initiation, with the possibility of recycling the monomer−template solution (Figure 2). The problem of confining polymer chain growth to the support surface and suppress it in solution can be solved by attaching the radical initiator in such a way that the radicals formed upon bond homolysis remain bound to the surface. Alternatively, the radical formed that is not attached to the surface should possess low reactivity or undergo rapid reaction to give an unreactive species. A further option is the use of physically adsorbed initiators capable of abstracting hydrogen radicals from the support.[22]

Here we report on composite MIPs prepared using azo initiators covalently bound or physically adsorbed to the surface. The materials can be prepared in a short time (1−2 h) and exhibit superior mass transfer properties and saturation capacities when compared to previously described monolith MIPs in liquid chromatography or when compared to grafted coatings prepared by the conventional "grafting to" procedure. These materials can be applied in HPLC as well as in capillary electrochromatography (CEC)[30] and they can be prepared using different template targets.

## Experimental Section

**Chemicals.** BOC-L-phenylalanine, *N,N′*-dicylcohexylcarbodiimide (DCC), trifluoroacetic acid, ethylene glycol dimethacrylate (EDMA), methacrylic acid (MAA), (3-aminopropyl)-triethoxysilane (APS), ethyl chloroformate and glycidoxypropyltrimethoxysilane (GPS) were obtained from Aldrich (Deisenhofen, Germany). EDMA containing polymerization inhibitor (100 ppm of the monomethyl ether of hydroquinone) was used as received whereas MAA was purified by distillation under reduced pressure. 1-Hydroxybenzotriazole hydrate (HOBt), 4,4′-azobis(4-cyanopentanoic acid) (ACPA), 3-aminoquinoline, ethyl acetate, methanol, and acetic acid (AcOH) were obtained from Fluka (Deisenhofen, Germany). Concentrated hydrochloric acid, chloroform, dichloromethane (DCM) and acetonitrile (ACN) were obtained from Merck (Darmstadt, Germany). BOC-D-phenylalanine was purchased from Bachem (Heidelberg, Germany). The templates L- and D-phenylalanine anilide (LPA, DPA) were synthesized following a previously described procedure[31] with slight modifications. Aniline was obtained from Aldrich. Anhydrous solvents dimethyl formamide (DMF), dimethyl sulfoxide (DMSO), toluene and tetrahydrofuran (THF) were purchased from Fluka and used as received. The silica research samples with average pore sizes of 1000 Å (Si1000), 300 Å (Si300), 100 Å (Si100) and the nonporous silica (SiNP) were supplied by Dr. D. Lubda from

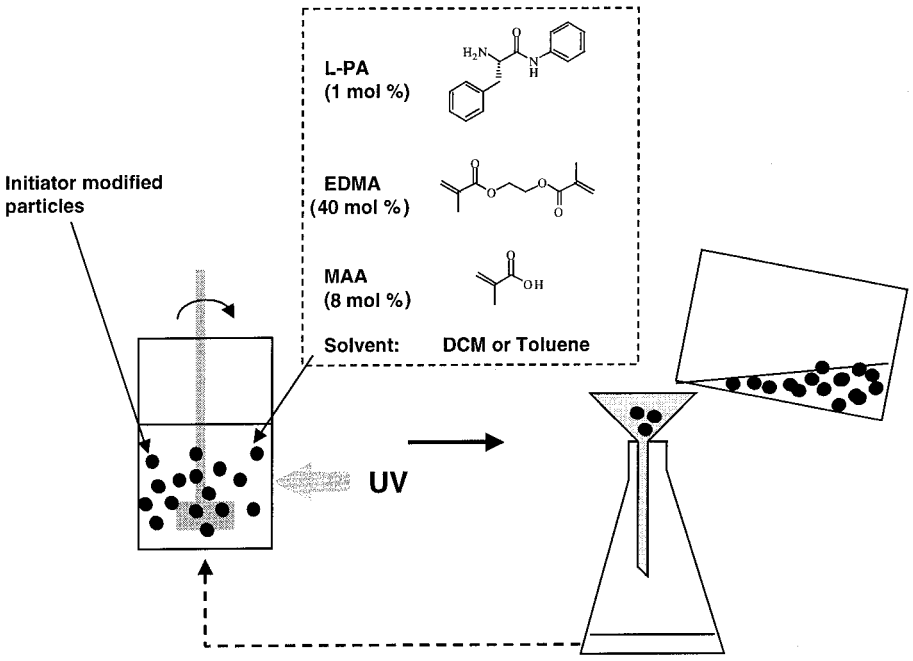


**Figure 2.** Protocol for grafting of imprinted polymer layers on support materials with recycling of the monomer solution.

Merck KGaA (Darmstadt). The amidine initiator 2,2′-azobis-(*N*,*N*′-dimethyleneisobutyramidine) (ADIA) was obtained from Wako Chemicals GmbH (Neuss, Germany).

**Apparatus.** The HPLC measurements were carried out on Hewlett-Packard HP 1050 and 1090 instruments (Agilent Technologies, Waldbronn, Germany). The fluorescent labeled silica particles were investigated using a LEICA DM R fluorescence microscope HC (Benzheim, Germany). Therefore the silica samples were prepared as described below. The grafting yields were estimated from elemental microanalysis obtained using a "CHN-rapid" HERAEUS analyzer (Hanau, Germany). FT-IR spectroscopy was performed using a MATTSON 2030 Galaxy Series FT-IR spectrometer (Madison, WI). The particle morphology, size and size distribution were determined using a LEO 1530 "Gemini" scanning electron microscope (LEO Elektronenmikroskopie GmbH, Oberkochen, Germany). The material was applied on a carbon support without gold-coating. The yield of grafted polymer was also determined using a TGA analyzer Linseis L81 (LINSEIS Germany, Selb, Germany). The samples were heated to 1000 °C with a heating rate of 10 °C/min. A platinum crucible was used as the reference. Nitrogen sorption measurements were performed using an AUTOSORP-6 (QUANTACHROM, Odelzhausen, Germany). Before measurement 100−150 mg of the samples were heated at 150 °C under high vacuum ($p <$ 0.003 Torr) for 14 h. The isotherms were measured with liquid nitrogen as adsorptive at 77 K. The yield of initiator immobilization was investigated using a NETZSCH DSC 204 (NETZSCH-Gerätebau GmbH Thermal Analysis, Selb, Germany).

**Initiator Modification of Silica Particles. Covalently Bound Initiator.** The porous Si 1000 (average particle diameter, $d_p = 5-10$ $\mu$m, specific surface area, $S = 33$ m$^2$/g), Si 300 ($d_p = 10$ $\mu$m, $S = 60$ m$^2$/g), nonporous (NP) silica ($d_p =$ 2.8 $\mu$m, $S = 0.33$ m$^2$/g), Si 100 ($d_p = 10$ $\mu$m, $S = 380$ m$^2$/g) were modified with the azoinitiator in two steps following a procedure described by Tsubokawa via GPS[32] and Revillon et al. via APS to give the initiatormodified support as shown in Figure 1.[26] GPS: During the modification described by Tsubokawa the silica is treated with GPS in toluene, followed by a reaction of the GPS-particles with ACPA and α-picoline in DMSO. APS: In the first step APS is immobilized on the surface of the silica particle and the product is then reacted with ACPA in the presence of ethyl chloroformate and triethylamine at −78 °C.

**Noncovalently Bound Initiator.** For the noncovalent attachment of an azoinitiator on porous silica, 2,2′-azobis(*N*,*N*′-dimethyleneisobutyramidine (ADIA) was used. For Si-ADIA 1 and 3, silica (3 g) and the initiator (0.7 mmol) were stirred for 2 h in chloroform (100 mL) at room temperature. The solvent was then evaporated and the silica dried in a vacuum oven at room temperature. For Si-ADIA 2 and 4 chloroform was replaced by water and the mixture stirred overnight. After filtration the particles were dried under vacuum at room temperature.

**Grafting Step.** The grafting was carried out in test tubes containing the initiator-modified particles (0.1 g) suspended by a nitrogen stream in a degassed solution of the monomers (MAA (0.068 mL) and EDMA (0.76 mL)), solvent (toluene or dichloromethane (1.12 mL)) and template (LPA (0.024 g)). For the HPLC evaluation, larger batches of the initiator-modified particles (0.5 g) and appropiate amounts of monomers, solvent and template were used. Prior to polymerization, the suspension was degassed by applying four freeze−thaw degassing cycles. The photochemical initiation was carried out by immersing the test tubes in a thermostated water bath at 15 °C and placing them near (ca. 5 cm) a high-pressure mercury vapor lamp (Philips, HPK 125 W) used as the UV light source. The samples were purged with nitrogen throughout the polymerization. After polymerization, the samples were extracted with methanol using a Soxhlet apparatus for 24 h.

**HPLC Measurements and Evaluation.** Unless otherwise mentioned, the particles were slurry packed into stainless steel columns (33 × 4 mm) using MeOH/$H_2O$ 80:20 (v/v) as pushing solvent. These were then evaluated using a water poor mobile phase consisting of ACN/$H_2O$/AcOH (v/v/v) with varying contents of ACN. Some of the columns were also evaluated using a water rich mobile phase: ACN/sodium acetate buffer, 0.01 M, pH 4.8: 70/30 (v/v). The flow rate was 1 mL/min, and 10 $\mu$L aliquots of a 1 mM solution and a 10 mM solution, both racemic mixtures and pure enantiomers, were injected. The elution was monitored at 242 nm. Upon a change in the mobile phase, the column was washed with the new mobile phase until a stable baseline was reached. The capacity factors ($k'_D$ and $k'_L$) and separation factor (α) were calculated using the following formula: $k'_D = (t_D - t_0)/t_0$; $k'_L = (t_L - t_0)/t_0$; $\alpha = k'_L/k'_D$, where $t_D$ is the retention time of the D enantiomer, $t_L$ is the retention time of the L enantiomer and $t_0$ the retention time of the void marker, acetone. The elution profiles were also evaluated with respect to the number of theoretical plates ($N$) the resolution factor $R_S$[54] and $f/g$, respectively. $N$ was calculated as $N = 5.55(t/t_{1/2})^2$, where $t_{1/2}$ is the peak width at half-height. In the latter case, $f$ is defined as the vertical distance between a line connecting the maxima of the peaks and the valley between the peaks and $g$ the vertical distance between the same line and the baseline.[55]

**Frontal Analysis.** Single-step frontal analysis was performed using solutions of either L-PA or D-PA in the mobile phase: ACN:AcOH:$H_2O$ 98.125:1.25:0.625 (v/v/v) at 25 °C and a flow rate of 1 mL/min. Eight solutions were prepared by diluting stock solutions (0.4 mmol/L) of the enantiomers with pure mobile phase with the following ratios: 99:1; 95:5; 90:10; 75:25; 60:40; 40:60; 20:80 and 0:100 (v/v). Before measurement, the columns were equilibrated with pure mobile phase for at least 30 min. The breakthrough curves were then recorded by a UV absorbance at 242 nm in the order of increasing concentrations. After measurement the column was washed with methanol for at least 20 min. The amount of solute needed to saturate the column was determined by the half-height method. Here, the resulting breakthrough curves were fitted using the sigmoidal fit followed by differentiation. The volume of the stationary phase, required for calculation of $q$ (concentration of solute in the stationary phase), was determined by subtraction of the dead volume (void marker: acetone) of the column from the volume of an empty column.

**Coupling of the Fluorescence Label.** The polymer modified silica (0.04 g), HOBt and DCC were mixed in dry DCM (20 mL) and stirred for 30 min before a solution of 3-aminoquinoline (3AQ) (1.1 eq. based on the theoretical amount of COOH groups of the polymer) in DCM was added dropwise. The solution was stirred for 60 h and filtered, and then the solid remaining was washed consecutively with DCM and ethyl acetate. The silica was dried under vacuum at 40 °C. Rehydroxylated silica was also treated under identical conditions as a reference.

**Reduced Batch Size Imprinting of Terbutylazine.** Two mother solutions were prepared according to the procedure described previously,[33] by mixing EDMA (3.8 mL, 20 mmol), MAA (0.34 mL, 4 mmol) and DCM (5.6 mL), all reagents purified prior to use. To one of the solutions terbutylazine (1 mmol) was also added (template mother solution). The mother solutions (120 $\mu$L) were dispensed into 1.5 mL glass vials together with ∼50 mg of Si1000 containing immobilized initiator (APS). All the vials were sonicated for 20 min, frozen with liquid nitrogen, degassed with nitrogen for 2 min, and finally transferred to a thermostated water bath (15 °C). The polymerization was then initiated by UV irradiation (vide supra) and the vials vigorously shaken at regular intervals during 1 h. Thereafter DCM (1 mL) was dispensed into each of the vials containing the blank and imprinted grafted polymers. The vials were then sonicated for 15 min and left standing overnight. After that the amount of the template released into solution was quantified by HPLC−UV using an external standard as described previously.[33] Glacial acetic acid (50 $\mu$L) was added and the concentration of the template in the supernatant was evaluated again after overnight equilibration. The supernatant was thereafter removed from each vial and all the polymers were washed three times with 1 mL of DCM/AcOH: 95/5 (v/v) and finally with DCM (1 mL). The rebinding experiment was then performed by addition of a

**Table 1. Area Density and Coverage of the Silanes and Azo Initiators Based on Elemental Analysis after Sequential Coupling to Silica Supports[d]**

| | | step 1 | | | | | step 2 | | | |
|---|---|---|---|---|---|---|---|---|---|---|
| modified support | support | % C | % N | area density[a] ($\mu$mol/m$^2$) | coverage[b] (%) | azoinitiator | % C[c] | % N[c] | area density[a] ($\mu$mol/m$^2$) | coverage[b] (%) |
| Si-APS-1a | Si1000 | 0.83 | 0.18 | 3.9 | 49 | ACPA | 1.30(0.47) | 0.33(0.15) | 0.81 | 10 |
| Si-APS-1b | Si1000 | 0.56 | 0.15 | 3.3 | 41 | ACPA | 0.96((0.40) | 0.28(0.13) | 0.70 | 8.8 |
| Si-APS-1c | Si1000 | 0.45 | 0.13 | 2.8 | 35 | ACPA | 0.93(0.48) | 0.28(0.15) | 0.81 | 10 |
| Si-APS-1d | Si1000 | 0.51 | 0.19 | 4.1 | 51 | ACPA | 1.07((0.56) | 0.27(0.08) | 0.43 (0.9) | 5.4 (11) |
| Si-APS-2 | Si300 | 0.93 | 0.29 | 3.4 | 43 | ACPA | 1.78(0.85) | 0.50(0.21) | 0.63 (1.1) | 7.9 (14) |
| Si-APS-3a | SiNP | 0.46 | 0.06 | | | ACPA | 0.85 | 0.03 | | |
| Si-APS-3b | SiNP | 0.52 | 0.06 | | | ACPA | 1.06 | 0.03 | | |
| Si-APS-4 | Si100 | 5.07 | 1.33 | 3.0 | 38 | ACPA | 6.19(1.12) | 1.71(0.38) | 0.2 | 2.5 |
| Si-ADIA-1a | Si1000 | | | | | ADIA | 0.56 | 0.28 | 1.0 | 12.5 |
| Si-ADIA-1b | Si1000 | | | | | ADIA | 0.49 | 0.28 | 1.0 (2.3) | 12.5 (29) |
| Si-ADIA-2 | Si1000 | | | | | ADIA | 0.30 | 0.15 | 0.53 | 6.7 |
| Si-ADIA-3a | Si300 | | | | | ADIA | 0.96 | 0.53 | 1.1 | 13.8 |
| Si-ADIA-3b | Si300 | | | | | ADIA | 0.67 | 0.38 | 0.79 | 9.9 |
| Si-ADIA-4 | Si300 | | | | | ADIA | 0.65 | 0.41 | 1.45 | 18.1 |
| Si-PMA | Si1000 | 0.70 | | 2.3 | 29 | | | | | |

[a] The area density ($D$) was calculated from the nitrogen content as $D = m_N/(M_N S)$, where $m_N$ = % N/(100 − (% N)$M_w/M_N$), $M_w$ = molecular weight of immobilized silane or azoinitiator (step 2), $M_N$ = weight of nitrogen per mole of immobilized species and S = specific surface area of the silica support. $M_w$ and $M_N$ were calculated assuming complete conversion of the silane. The specific surface areas of the silica supports were as follows: Si1000, 33 m$^2$/g; Si300, 60 m$^2$/g; Si100, 380 m$^2$/g; SiNP, 0.34 m$^2$/g. The values in parentheses were obtained from DSC. $D$ was here calculated as the ratio of the integral of the decomposition exotherm ($I_{dec}$, kJ/g) to the enthalpy of decomposition of the pure initiator ($\Delta H_{dec}$) and $S$ as $D = I_{dec}/(\Delta H_{dec} S)$. The temperature ($T_{dec}$) and enthalpy of the decomposition exotherm were as follows: for pure ACPA: $T_{dec}$ = 128−131 °C, $\Delta H_{dec}$ = 152.3 kJ/mol; pure ADIA, $T_{dec}$ = 112−132 °C, $\Delta H_{dec}$ = 131.1 kJ/mol; Si-APS-1d, $T_{dec}$ = 113 °C; Si-APS-2, $T_{dec}$ = 116 °C; Si-ADIA-1b, $T_{dec}$ = 136 °C. [b] The coverage ($C$) was calculated as C = 100 × $D$/8, assuming a maximum silanol group density of 8 $\mu$mol/m$^2$. Values in parentheses represent data obtained from the DSC measurements. [c] The values in parentheses show the increase in nitrogen content upon initiator immobilization. These were used to calculate the area density of the azo initiator. [d] The immobilizations were performed as described in the Experimental Section and in Figure 1 in one or two steps and the modified supports analyzed by elemental analysis of carbon and nitrogen or by differential scanning calorimetry (DSC) based on the exotherm of initiator decomposition.

solution of terbutylazine (1 mL, 0.1 mM) in DCM. The vials were sonicated for 5 min and then allowed to stand for 24 h. Thereafter the concentration of free (unbound) terbutylazine was determined by reversed-phase HPLC.

## Results and Discussion

**Surface Attachment of Free Radical Initiator.** Initiating polymerizations from the surfaces of solids involves a number of parameters additional to those for the homogeneous solution case; each parameter needs to be known and its importance assessed. These include the nature of initiator attachment, the density of initiating groups,[28] the ability of the monomer mixture to efficiently wet the surface[34] and monomer partitioning effects, the latter being particularly a problem in copolymerizations leading to deviation from reactivities derived from homogeneous solution.

The methods for immobilizing free radical initiators on solid supports are distinguished in the nature of their attachment (covalent or noncovalent) and whether initiator decomposition leads to a mobile initiating radical or only surface confined radicals.[34] Covalent immobilization of the initiator involves several synthetic steps but leads to a stable attachment of the resulting polymer to the surface. This technique was introduced by Challa et al.[35] and is the most commonly employed to initiate polymerizations from solids. The other alternative, physical adsorption of the initiator, was introduced by Dekking et al.[36,37] for the grafting of vinyl polymers onto the surface of clay and has recently been used by Suter et al. for grafting of polystyrene to mica surfaces.[38] Although perhaps technically more straightfoward the initiator or polymer may be displaced by acids or bases competing with the initiator for the surface adsorption sites. This may restrict the approach concerning the use of acidic or basic functional monomers.

We chose to assess both covalent and noncovalent systems in our study. First we assessed the covalent route. The original method introduced by Guyot et al.[39] and Tsubokawa et al.[32,40] comprises in two successive surface reactions, the first being the reaction of the free silanol groups on the surface with (3-aminopropyl)-triethoxysilane (APS) or trimethoxyglycidoxypropylsilane (GPS) followed by reaction of the amino or epoxy groups with an azoinitiator such as azobis(cyanopentanoic acid) (ACPA) leading to the formation of an amide or ester bond between the surface and the azoinitiator, respectively (Figure 1). These coupling reactions were applied to support materials with different morphologies and pore systems. To reduce the risks of pore blocking, our initial work focused on the use of wide pore silica particles with an average pore size of 100 nm and particle diameter of 5−10 $\mu$m. We then anticipated that the resulting optimised method could be transferred to other support morphologies.[41]

Prior to the first modification step, the silica surface was rehydroxylated according to standard procedures. This is known to result in a maximum density of free silanol groups of ca. 8 $\mu$mol/m$^2$.[42] The yield in each step was then calculated based on results obtained by elemental analysis or thermal gravimetric analysis (TGA)/differential scanning calorimetry (DSC). As can be seen in Table 1, a maximum of half of the silanol groups reacted with APS or GPS in the first silanization step. This is in agreement with the results obtained by Guyot et al.[39] and has been attributed to bridging of two silanol groups by one organosilane moiety or, in the case of APS, the occurrence of strong hydrogen bonds between amino groups of the immobilized APS and neighboring silanol groups. The subsequent step was then the attachment of ACPA to these surfaces. On the basis of the increase in nitrogen content, a maximum

area density of 0.7−0.8 $\mu$mol/m$^2$ was calculated. This corresponds to a minimum conversion[43] of ca. 20% of the surface amino groups and an overall conversion of the silanol groups of ca. 10%. This coverage constitutes about a third of the maximum coverage obtained using presynthesized azosilanes. It is questionable whether high surface coverage is beneficial for the grafting of cross-linked polymers. With high coverages recombination of initiator molecules or primary chains becomes more frequent, especially under conditions where the initiator decomposition is fast, such as by photoinduced decomposition or thermally induced decomposition at high temperatures.[28]

The presence of the initiator was indicated by the IR spectra of a sample of Si-APS-1. Thus, bands corresponding to the stretching vibrations of the amide and carboxylic acid groups of the initiator were seen in the sample of the initiator-modified silica.[44] To study the influence of the initiator area density on the polymer grafting, two modified GPS surfaces were prepared containing different amounts of ACPA. As a further comparison we also immobilized methacrylate groups for the grafting of polymers *to* the surface.

The noncovalent approach was assessed by adsorbing a strongly basic amidine-containing initiator to bare silica. These initiators have proven useful for both thermal and photopolymerization of water soluble monomers in water, for emulsion polymerizations and for graft polymerizations.[37] In the latter examples, they are adsorbed onto anionic substrates and remain adsorbed due to their cationic nature over a large pH interval. Homolysis leads to the formation of two cationic radicals and we reasoned that their limited solubility in organic solvents would prevent desorption from an anionic surface upon immersing the modified surface in the monomer mixtures used for grafting. In the preferred method the initiator (free base form) was adsorbed to bare silica particles from chloroform, the particles washed and dried and then subjected to elemental analysis. As can be seen in Table 1, this resulted in a reproducible and slightly higher coverage (ca. 1 $\mu$mol/m$^2$) than was obtained from the two-step procedure. Again, the extent of one-point relative to two-point attachment is not possible to assess, but in view of the minimum distance between neighboring silanol groups (ca. 5 Å) relative to the spacing between the amidine groups,[45] bridging as suggested in Figure 1 should be possible.

A general note should be made concerning the two-point immobilization of the initiator. Photoinitiated decomposition of azo initiators is believed to occur through photoinduced trans to cis isomerization and thermal decomposition of the cis isomer.[46] Obviously, this process may be hindered upon attaching the initiator at both ends (although no effect was observed by Dekking for bisamidines sandwiched between clay sheets[36]). To investigate this, the decomposition of the initiators was examined by differential scanning calorimetry. The exotherm of initiator decomposition has previously been used to quantify the amount of grafted initiator assuming an enthalpy of decomposition identical to that measured for the pure initiator.[28] As seen in Table 1, the values estimated by this method were somewhat higher, but proportional, to those obtained by elemental analysis. To investigate the photoinduced decomposition, samples of the initiator-modified particles were immersed in the polymerization solvent (toluene) and irradiated for the same durations as applied in the grafting experiments. Thereafter, the samples were investigated again with DSC. The integral of the decomposition exotherm decreased rapidly and was no longer measurable after an irradiation time of 15 min. This rate agreed roughly with the one measured for the initiator in solution, and thus the immobilization did not appear to affect the decomposition kinetics significantly.

**Kinetics of Polymer Grafting.** Reactions occurring at solid−liquid interfaces require that the substrates in solution can access the reactive groups on the solid surface. This requires a low surface tension, resulting in complete wetting of the surface by the reaction medium.[42,47] Prior to attempting the grafting of polymers to solid supports, it is thus important to investigate the wettability of the surface by the monomer mixture. A qualitative technique is to investigate the degree of particle agglomeration when the particles are immersed in the corresponding liquid. The initiator-modified particles were thus immersed in the monomer mixture (using toluene as solvent), water or *n*-hexane and the samples studied by optical microscopy. Whereas pronounced agglomeration was observed in water and *n*-hexane, the particles seemed to be better dispersed in the monomer mixture. This indicates that the surface in this case is well wetted by polar organic solvents, such as the monomer mixture. Depending on the type of functional monomer used additional post-modification steps (e.g., end capping) may be required.

The grafting experiments were then performed at a scale allowing the product to be analyzed by solid state characterization techniques (0.1 g) (Figure 3) or by liquid chromatography (0.5 g) (Table 2). As a model system we chose L-PA as a template, EDMA as cross-linker, and MAA as functional monomer, with dichloromethane or toluene as porogenic solvents. The corresponding monolithic materials have been thoroughly studied with respect to thermodynamics and mass transfer properties,[5,48,49] polymer structure and morphology[50,51] and the molecular recognition mechanism[52] and are thus well suited as bench marks for this study. Photoinitiation was used throughout the experiments since this is known to lead rapidly to high conversions and to result in MIPs with an enhanced performance in chromatography. After careful removal of oxygen[53] from the slurry of initiator-modified particles in the monomer mixture, the samples were immersed in a thermostated water bath and irradiated with a high-pressure Hg lamp under continuous purging with nitrogen. Samples were withdrawn at regular time intervals; these were washed, dried and investigated for their carbon content by elemental analysis and by infrared spectroscopy. In Figure 3 the corresponding time course of the grafting is shown as plots of the carbon content and the intensity of the carbonyl stretch at 1730 cm$^{-1}$ normalized to the $SiO_2$ matrix vibration at 470 cm$^{-1}$. The resulting plots were essentially superimposable showing that the IR-method can be used to estimate the grafting yield in this system. The amount of grafted polymer increases continuously throughout the initial 2 h of irradiation. Differences are seen depending on the type and density of initiator on the surface and on the kind of solvent used. Thus, polymerization was more rapid using dichloromethane as solvent,where a grafted amount corresponding to an average layer thickness, assuming formation of a ho-

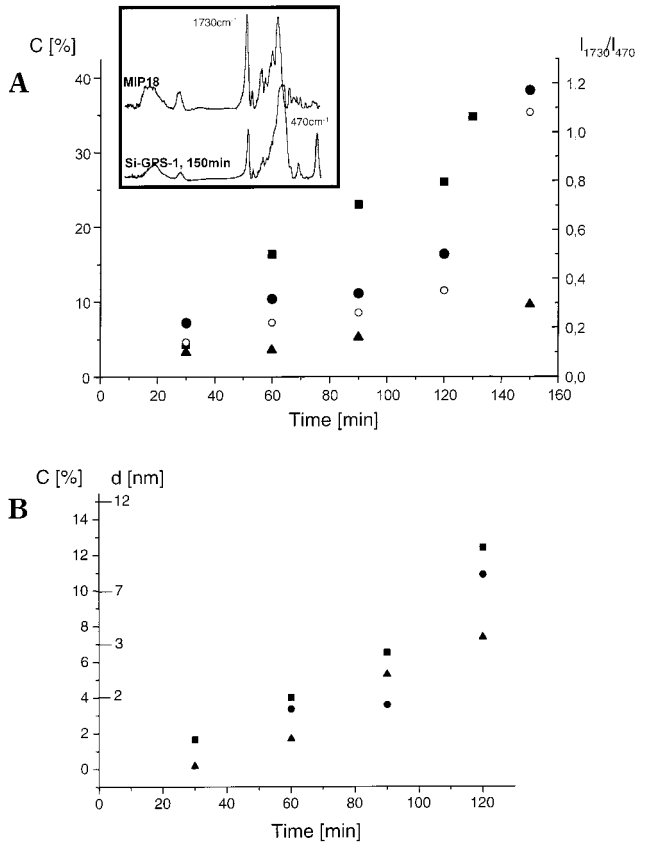


**Figure 3.** Time course of the graft copolymerization of EDMA and MAA in absence (A) and presence (B) of template using various initiator-modified support materials (0.1 g) and solvents. The data are plotted as the carbon content obtained by elemental analysis (C (%)) vs time. The following supports were used. (A) Si-GPS (Si1000) with an area density of immobilized initiator of 0.65 (Si-GPS-1) and 0.27$\mu$mol/m$^2$ (Si-GPS-2). Key: (■) Si-GPS-1 in DCM; (●) Si-GPS-1 in toluene; (▲) Si-GPS-2 in toluene. For the grafting on Si-GPS-1 in toluene the ratio of the integral of the band at 1730 cm$^{-1}$ to the integral of the band at 470 cm$^{-1}$ ($I_{1730}/I_{470}$) (see inserted spectra of Si-GPS and a polymer prepared following the conventional monolith protocol (MIP 18)) obtained by infrared spectroscopy is also shown (○). (B) Key: (■) Si-APS-1a in toluene; (●) Si-APS-1c in toluene; (▲) Si-ADIA-1a in toluene. The surface areas, obtained from nitrogen BET analysis, were found between 30 and 34 m$^2$/g. The average thickness of a homogeneous grafted layer ($d$) was calculated as follows: $d = m_C M_w/(M_C DS) \times 10^4$ (Å), where $m_C$ = % C/(100 − (% C)$M_w/M_C$) = weight of carbon of the grafted polymer per gram of bare silica support, $M_w$ = weighted average molecular weight of the grafted polymer assuming stoichiometric incorporation of the reacting monomers. $M_C$ = weighted average molecular weight of the carbon fraction of the grafted polymer. $D$ = weighted average density of the monomers (g/mL). $S$ = specific surface area of the bare support resin (m$^2$/g).

mogeneous film on the surface and with no compensation for volume shrinkage upon polymerization, of ca. 10 nm was reached after 60 min irradiation time. Using toluene as solvent, the growth was slower and the rate increased with increasing surface density of immobilized initiator, the latter being in agreement with previous observations for thermally initated polymerizations.[28] The solvent effect may be due to light dispersion caused by poor matching of refractive indices or different ability of the solvents to wet the surface of the support.

By careful control of conditions, the grafting kinetics were reproducible during the initial phase of the polymerization (Figure 3B). At higher grafting amounts (15−25% C), observed at longer polymerization times (>90 min), a larger scatter of the data was seen, probably as a result of sample heterogeneity due to particle agglomeration and gelation in solution. This problem was reduced by the use of monomers containing known amounts of polymerization inhibitors.

**Characterization of Grafted Polymer Layers.** After polymerization, the particles were subjected to extensive extraction with methanol in a Soxhlet apparatus, dried and subsequently characterized by TGA, SEM and fluorescence microscopy. The results of the TGA showed mass loss curves typical for monolithic cross-linked polymers of this type with an onset of mass loss at about 240 °C (Table 3). For lower grafted amounts, the mass loss agreed closely with the amount of grafted polymer estimated on the basis of elemental analysis, indicating that any of the techniques can be used to monitor the amount of grafted polymer. The discrepancy between the data at higher grafted amounts is likely due to sample heterogeneity. A higher temperature for the onset of mass loss (258 °C) was obtained for the materials containing the lowest grafted amount. This may indicate that the film formed in the initial stages of the polymerization is stabilized by the silica support (the average film thickness in this case is just 1.8 nm).

Unfortunately, the scanning electron micrographs of the porous materials provide only very limited evidence for the nature of the films. This is due to a pronounced heterogeneity with respect to the native particle porosity. Thus, within one sample of the native Si1000, particles showing the expected porosity were mixed with particles showing essentially no porosity. Nevertheless an increasing amount of polymer on the outer surface of the particles with increasing carbon content from elemental analysis was apperent (data not shown). This appeared more clearly from the SEM of the nonporous particles (Figure 4). Here a pronounced difference is seen when comparing the native and the polymer modified particles. It is clearly seen that the polymer covers the particle surface, although solution growth has also occurred, as seen in the occurrence of some irregularly shaped particles. At higher grafting levels, these particles attach to each other forming larger porous agglomerates (>100 $\mu$m) composed of nonporous silica particles (2.8 $\mu$m) held together by a weblike polymer structure with micron sized interstitial pores. This suggests that the grafting of polymer in this case may play two roles, first to introduce surface functional properties and second to immobilize the microparticles for instance in columns or capillaries.

Additional evidence for the quality and homogeneity of the grafted polymer films was obtained by fluorescence microscopy of particles that had been previously labeled with the fluorescent dye 3-aminoquinoline (3-AQ). Particles containing different amounts of grafted polymer were reacted under amide coupling conditions with the dye, which was added in excess to the theoretical number of incorporated carboxylic acid groups. The coupling yield of 3-AQ and the fluorescent micrographs are informative of the accessibility and homogeneity of the polymer films. The former was estimated based on elemental analysis and showed a decrease with increasing amount of grafted polymer. Thus, a quantitative yield was obtained only for the particles with a carbon content of 5%, corresponding to an average film thickness of 2.5 nm. This shows that the carboxylic acid

**Table 2. Synthesis Conditions and Characterization of Grafted Molecularly Imprinted Polymers (MIPs) Used as HPLC Chiral Stationary Phases[a]**

| grafted polymer | initiator-modified support | silica support | reaction time (min) | % C | % N before extraction | % N after extraction | footnote |
|---|---|---|---|---|---|---|---|
| MIP1 | Si-APS-1c | Si1000 | 90 | 3.6 | | 0.15 | |
| MIP2 | Si-APS-1b | Si1000 | 60 | 6.2 | | 0.25 | |
| MIP3 | Si-APS-1b | Si1000 | 120 | 11.9 | 0.33 | 0.19 | |
| MIP4 | Si-APS-1c | Si1000 | 120 | 10.9 | 0.28 | 0.16 | |
| MIP5 | Si-APS-1c | Si1000 | 105 | 18 | | 0.13 | |
| MIP6 | Si-APS-1c | Si1000 | 90 | 7.4 | | 0.16 | *b* |
| MIP7 | Si-APS-1c | Si1000 | 60 | 11.7 | | 0.15 | *b* |
| MIP8 | Si-APS-2 | Si300 | 60 | 8.2 | 0.44 | 0.37 | |
| NIP8 | Si-APS-2 | Si300 | 60 | 10.4 | | 0.36 | |
| MIP9 | Si-APS-2 | Si300 | 30 | 5.0 | 0.56 | 0.43 | |
| MIP10 | Si-APS-2 | Si300 | 70 | 8.2 | 0.58 | 0.41 | |
| MIP11 | Si-ADIA-3a | Si300 | 40 | 7.6 | | 0.06 | |
| MIP12 | Si-APS-3b | SiNP | 30 | 1.3 | 0.08 | 0.03 | |
| MIP13 | Si-APS-3b | SiNP | 50 | 5.8 | | 0.02 | |
| MIP14 | Si-APS-4 | Si100 | 15 | 16.0 | | 1.55 | *b* |
| MIP15 | Si-PMA | Si1000 | 48 h | 13.4 | | | *c* |
| MIP16 | Si-PMA | Si1000 | 24 h | 17.2 | | | *c* |

[a] Unless otherwise mentioned, the materials were prepared using initiator or monomer modified silica supports in batches of 0.5 g using toluene as solvent and L-PA as template as described in the Experimental Section. The amount of removed template can be estimated from the loss of nitrogen upon extraction. Assuming a stoichiometric incorporation of the template and the monomers in the grafted layer, the weight of nitrogen contributed by the template corresponds to 0.54% of the weight of carbon of the grafted polymer. This value is below the loss in nitrogen upon extraction indicating a high recovery of template. [b] Materials prepared using DCM as solvent. [c] Materials prepared using monomer-modified silica supports by thermal polymerization (MIP15) or photochemical polymerization (MIP16) using 10 g of support material. The specific surface areas obtained by BET analysis of these materials were 165 and 138 $m^2/g$, respectively. NIP = nonimprinted polymer prepared in the absence of template.

**Table 3. Comparison of the Amount of Grafted Polymer Based on Elemental Analysis (EA) and Thermal Gravimetric Analysis (TGA)[a]**

| reaction time (min) | % C | onset temp (°C) | graft yield (%) TGA | graft yield (%) EA | solvent |
|---|---|---|---|---|---|
| 30 | 4.3 | 258.4 | 7 | 7 | a |
| 60 | 16.3 | 232.5 | 21 | 28 | a |
| 90 | 22.9 | 242.7 | 27 | 39 | a |
| 90 | 11.1 | 238.3 | 16 | 19 | b |

[a] The grafting was performed in batches of 0.1 g and in absence of template using the initiator modified silica support Si-GPS-1 (Si1000) with an estimated area density of immobilized initiator of 0.65 $\mu$mol/$m^2$. The procedure described in the Experimental Section was followed using either DCM (a) or toluene (b) as solvents.

groups in the particles with higher graft densities are less accessible. Assuming a homogeneous film, increasing graft density will lead to a more hindered diffusion and a decrease in the reactivity of the carboxylic acid groups. At some point this may cause complete blocking of the pores. The fluorescence micrographs (Figure 5) support this explanation.

In these pictures, the labeled particles were soaked in dichloromethane and appear blue due to the fluorescence emission (387 nm) of the label. The samples appeared different both with respect to the variations of the intensity between the particles of one sample and with respect to the fluorescence intensity of a single particle. For the particles with the lowest grafting density, the particles fluoresced with approximately the same intensity, and the label appeared to be evenly distributed within the particle. However, for the particles with higher graft densities a large inter- and intraparticle variation in intensity was observed. In contrast to the low density particles, many of the particles exhibited a higher fluorescent intensity near the particle periphery, indicating poorer accessibility to the particle interior. This possibly reflects the existence of blocked pores. In conclusion, the particles with the lowest graft density exhibit relatively homogeneous films and the most accessible binding sites. It should also be mentioned that this post-labeling technique offers a convenient means of investigating the homogeneity of grafted polymer films.

**Characterization of the Particles in the Chromatographic Mode.** Imprinted polymer modified particles were prepared using silica particles of different porosities and sizes and at a batch size that would provide enough material for their evaluation as stationary phases in chromatography (Table 2). The particles were then slurry packed into short columns (33 × 4 mm) and evaluated initially in water poor (>92% (v/v) acetonitrile) mobile phases, containing acetic acid/water (2/1, v/v) as additive, for their ability to resolve and separate the enantiomers of the racemate of the template (D,L-PA). The resulting elution profiles were evaluated with respect to the retention of the two enantiomers, determined as the capacity factor (k′), the enantioselectivity, determined as the separation factor ($\alpha = k'_L/k'_D$), the column efficiency, determined as the number of theoretical plates ($N$) and the resolution, determined as the resolution factors $R_S$[54] or $f/g$[55] (in view of the asymmetric peaks the resolution factor $f/g$ reflects best the baseline-related resolution).

**Evaluation in Aqueous Poor Mobile Phases:** All columns packed with imprinted material showed reso-

**Scheme 1**

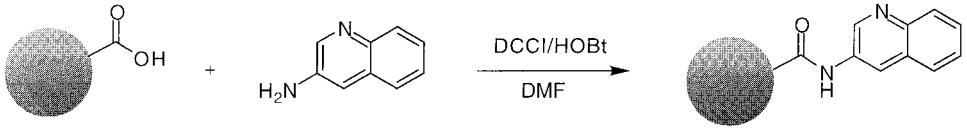

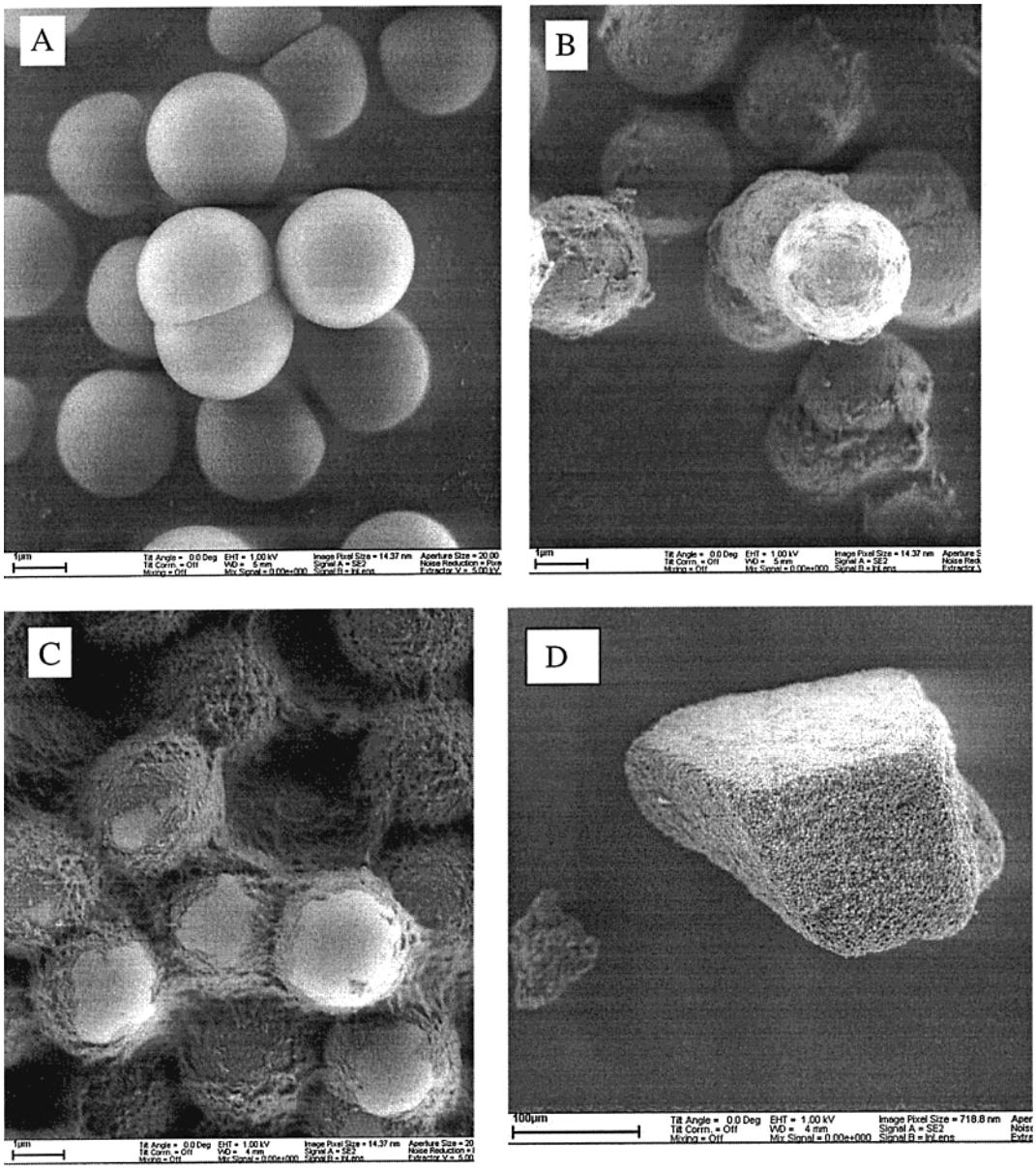


**Figure 4.** Scanning electron micrographs of the following samples: (A) unmodified nonporous $SiO_2$ particles (SiNP) with an average particle diameter of 2.8 $\mu$m; (B) Si-APS-3a with a grafted polymer containing 3.6% carbon; (C, D) Si-APS-3a with a grafted polymer containing 16% carbon. The materials were prepared using toluene as solvent and in absence of template except for micrographs C and D that were prepared using DCM as solvent.

lution of the racemate, the extent depending on the graft density, the solvent used, the support porosity and the technique used to immobilize the intiator. In Figure 6, the data have been represented in 3D format, with the average film thickness (assuming a homogeneous film) and the amount of acetic acid/water as variables, and in parts A and B of Figure 7, the corresponding elution profiles in one of the mobile phases are seen.

The capacity factor, separation factor and resolution ($f/g$) increased with increasing film thickness to reach a maximum at a film thickness of ca. 7.0 nm. For the grafting performed in toluene, the separation and resolution dropped for larger grafted amounts. This agrees with the trend observed by fluorescence microscopy, showing increasing heterogeneity and decreasing accessibility with increasing graft density. The associated decrease in column efficiency, reflected in the number of theoretical plates of the void marker acetone, supports this conclusion. The retention decreased as expected with increasing amount of modifier in the mobile phase[52] and, at 8% modifier, only the material with the 7.0 nm film gave separation and resolution of the enantiomers. Thus, less modifier is needed to completely suppress the retention and resolution when compared with the conventional monolith materials. The latter give best separation using a mobile phase containing 8% modifier.[51] This reflects the concentration of accessible carboxylic acid groups in the stationary phase. With a carbon content of ca. 12%, the organic portion of the stationary phase constitutes approximately 20% that of a stationary phase consisting of standard imprinted materials. The sample load capacity appears to follow the same trend. Thus, the elution profile of a 100 nmol injection of racemate on MIP3 (with an average film thickness $d = 7.0$ nm) appeared similar to the profile obtained upon injection of 10 nmol on MIP1 ($d = 1.8$ nm). A similar observation was made for the 30 nm pore size material, which possessed ca. a 2× larger surface area. Thus, the retention and separation factor obtained using MIP8 ($d = 2.5$ nm) lay

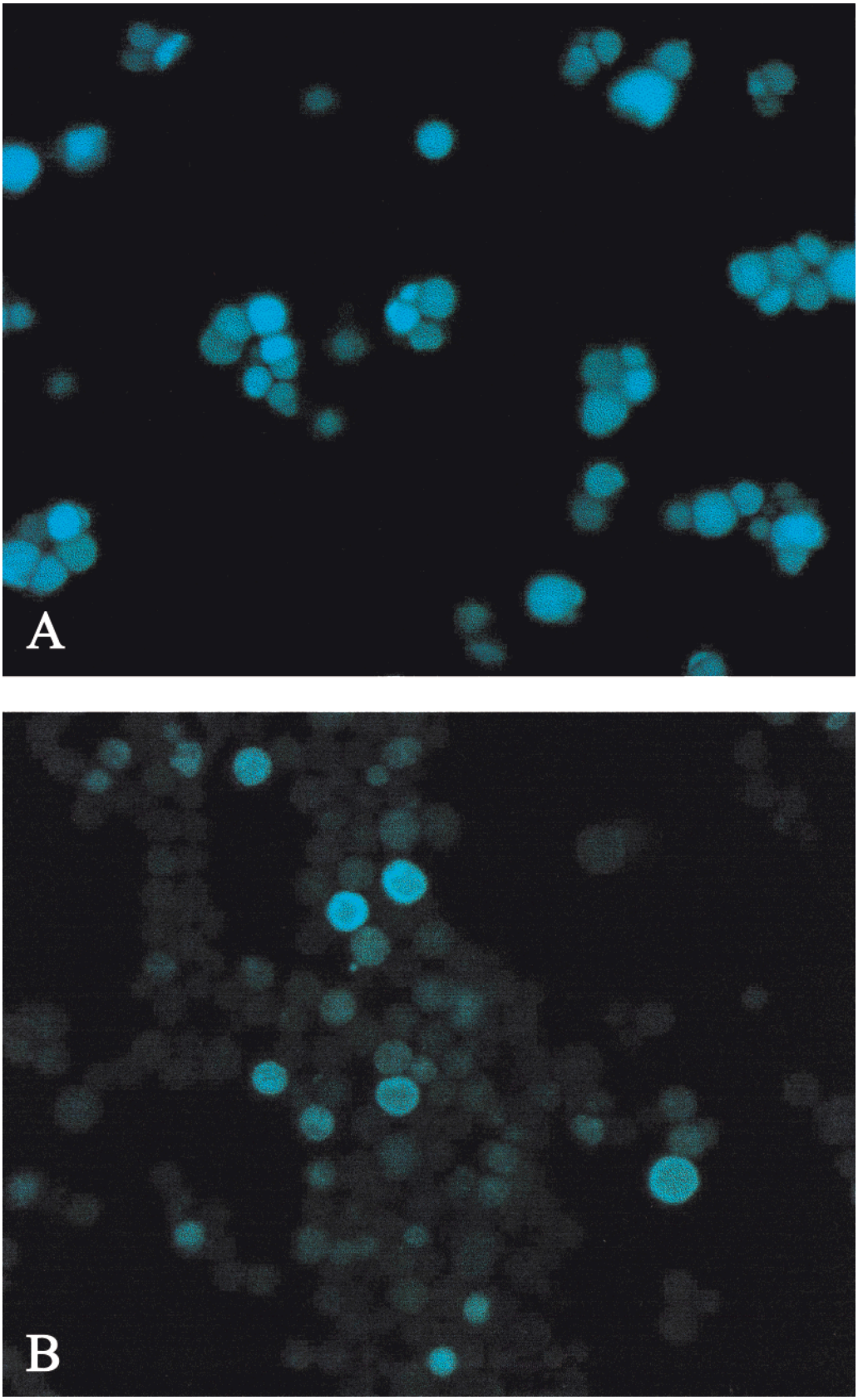


**Figure 5.** Fluorescence micrographs (40× magnification) of 3-aminoquinoline-treated materials. Si-GPS-1 with a grafted polymer containing 5% carbon (A) and 16% carbon (B). The materials were prepared in absence of template using toluene as solvent. The coupling of 3-aminoquinoline (3-AQ) was carried out as shown in Scheme 1 and as described in the Experimental Section. The yield of coupling of 3-AQ with the surface carboxylic acid groups, based on elemental analysis of N, were for the different carbon contents as follows: 5% C, ~100%; 16% C, 43%; 26% C, 46%. The yields were calculated assuming a stoichiometric incorporation of the monomers.

between those obtained on MIP2 ($d$ = 3.3 nm) and MIP3 ($d$ = 7.0 nm).

Although the retention decreased with increasing amount of modifier, the separation and resolution did

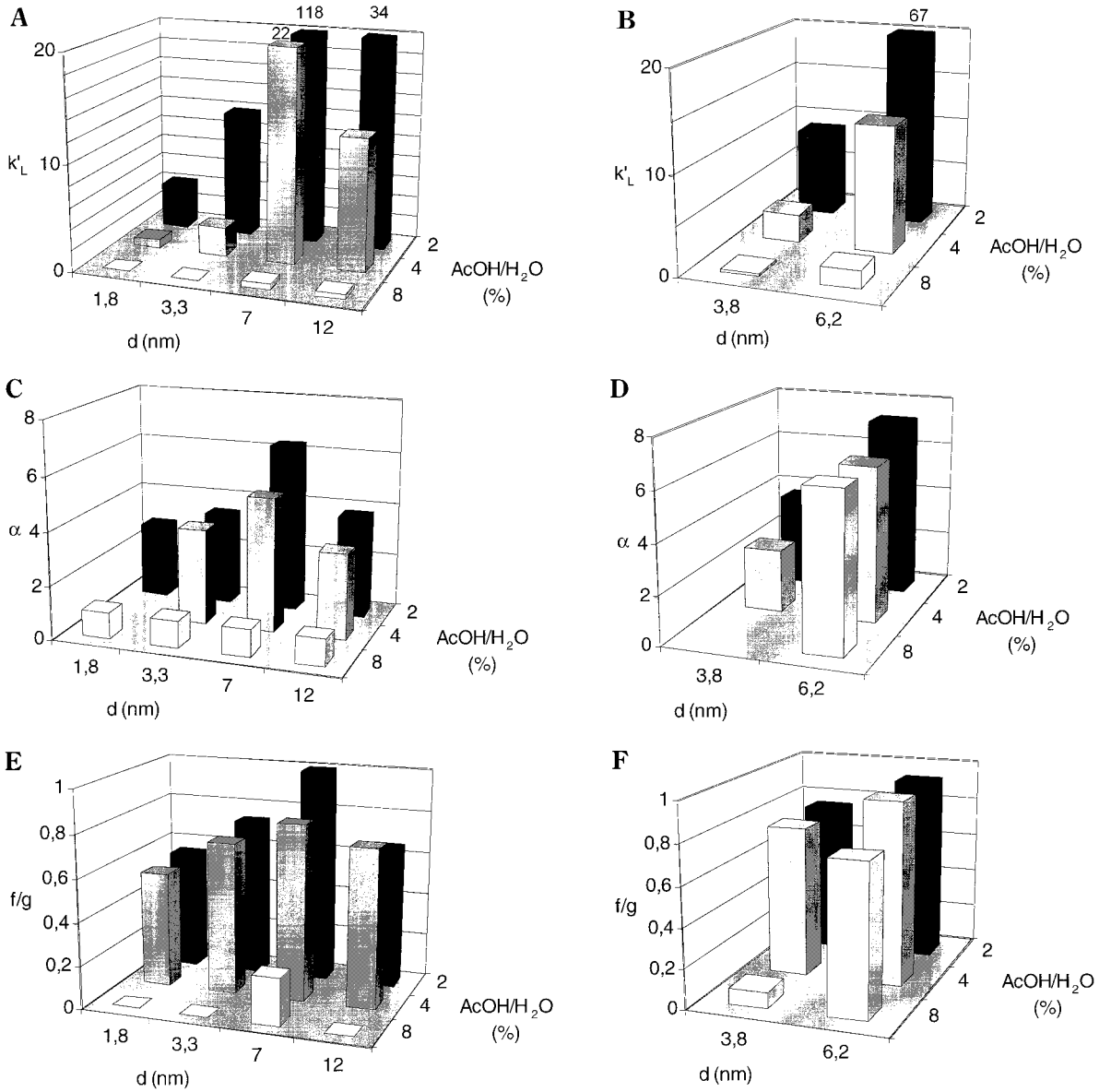


**Figure 6.** Results of the chromatographic evaluation of the imprinted materials plotted in 3D format. Materials MIP1, -2, -3, -5, -6, and -7 with average layer thicknesses ($d$) of 1.8, 3.3, 7.0, 12.0, 3.8, and 6.2 nm were packed in columns (33 × 4 mm) and evaluated by injecting D,L-PA (10 nmol) using mobile phases consisting of ACN containing various amounts of AcOH/$H_2O$:2/1 (v/v). The graphs show the capacity factor ($k'_L$) of L-PA (A, B), the separation factor ($\alpha$) (C, D), the resolution factor ($f/g$) (E, F) on MIP1−5 (A,C,E) and MIP6,7 (prepared using DCM as solvent) (B, D, F). In parts A and B, the capacity factors that fell outside the plotted range have been indicated. Some of the separation factors in parts C and D are missing due to elution of D-PA close to the void peak. The retention times in minutes were here as follows: MIP1 at 4% HOAc, $t_D = 0.54$, $t_L = 0.96$; MIP3 at 8% HOAc, $t_D = 0.45$, $t_L = 0.71$; MIP6 at 8% HOAc, $t_D = 0.51$, $t_L = 0.63$.

not change markedly up to 4% modifier.[52] In this context, the results of the particles with the thinner grafted films are of particular interest. In the water poor mobile phases, the materials with the thinnest films (MIP1, 1.8 nm; MIP14, 0.8 nm) showed relatively poor resolution of the enantiomers. However, the material with the 3.3 nm film exhibited good resolution, combined with elution of both enantiomers in less than 5 min (Figures 6 and 7A). Performing the grafting on support particles with smaller pores (Si300, 30 nm; Si100, 10 nm) resulted in similar chromatographic performance as observed for the 100 nm pore size material.

The solvent used during grafting also had an influence on the chromatographic properties. It is known that monolithic MIPs prepared using dichloromethane exhibit higher chromatographic efficiency than those prepared using toluene.[50] These materials also have a different dry state morphology, the former being of the gel type, with high swelling factor and the latter permanently porous with low swelling factor. Also, in the case of the grafted polymers, the materials prepared using DCM as solvent performed slightly better. As discussed above this may reflect differences in light dispersion, affecting in turn the kinetics of grafting, or the ability of the solvent to wet the initiator-modified surface.

**Evaluation in Water-Rich Mobile Phases.** A dramatic improvement in efficiency was observed upon changing to a water-rich mobile phase. Figure 7C shows a striking example of the enhanced efficiency observed for the thin film materials. Thus, on a column packed with Si100 coated with a 0.8 nm film the racemate could now be baseline resolved within a 5-min period with a separation factor of 6.3. This is mainly due to the

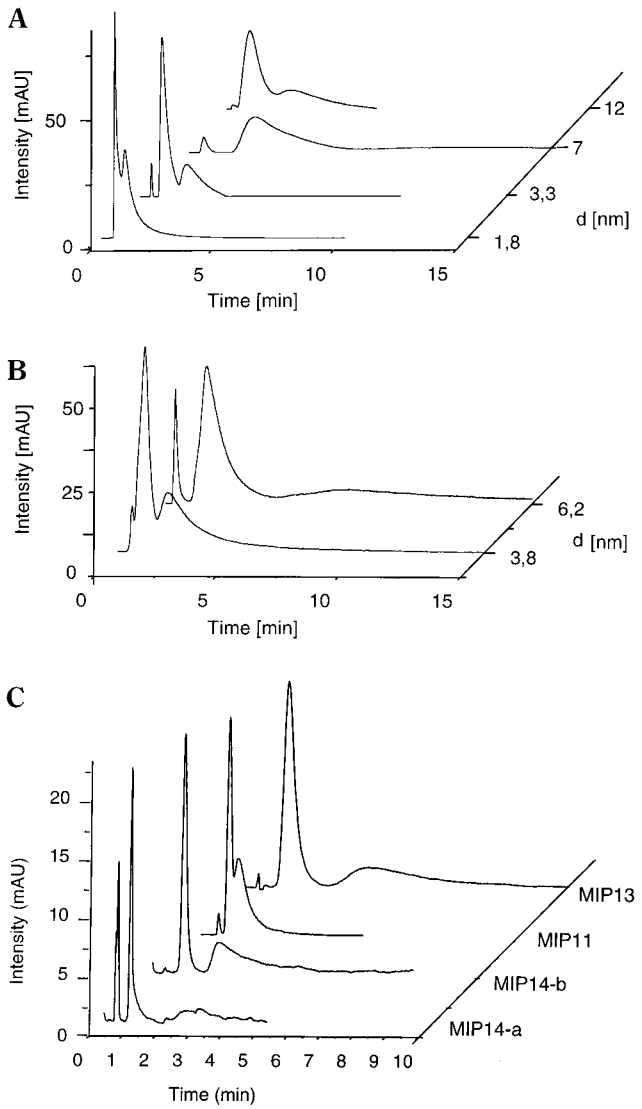


**Figure 7.** Elution profiles of (A) D,L-PA injected (10 $\mu$L of a 1 mM solution) on columns (33 × 4 mm) packed with MIP1, -2, -3, and -5 imprinted with L-PA using toluene as solvent and with average layer thicknesses of 1.8, 3.3, 7.0, and 12.0 nm. Mobile phase: ACN containing 4% of AcOH/$H_2O$: 2/1 as modifier. (B) As in part A but with MIP6 and MIP7 as stationary phases with average layer thicknesses of 3.8 and 6.2 nm, as stationary phases. MIP6 and MIP7 were prepared using DCM as solvent. (C) Elution profiles of D,L-PA injected (10 $\mu$L of a 0.05mM (MIP14a, MIP11) or 0.1 mM (MIP14b, MIP13) solution) on columns (33 × 4 mm) packed with MIP14 (Si100 with an average layer thickness of 0.8 nm), MIP13 (SiNP) or MIP11 (prepared by noncovalent immobilization of the initiator). The mobile phase was in this case ACN/sodium acetate buffer, 0.01 M, pH 4.8: 70/30 (v/v). The first eluting peak observed for MIP14-a is due to breakthrough of both enantiomers.

pronounced sharpening of the peak corresponding to the antipode of the template. The plate number obtained for this peak, 24000/*m*, at a low sample load (0.5 nmol of racemate) implies that the nonselective resistance to mass transfer, typically associated with MIPs, has here been largely overcome. This becomes clear when a comparison is made with the conventional L-PA MIP columns that exhibit plate numbers <2000/*m* for the D-enantiomer.[48] Interestingly the template peak exhibited only a slight sharpenening with a plate number of ca. 700/*m*. Thus the major contributions to the dispersion of this peak are factors related to the templated sites per se (e.g., site hetereogeneity, slow desorption).[48,56] This is further supported by the lack of significant improvements using the nonporous supports (Figure 7C), where slow mass transfer due to intraparticle pore diffusion is excluded.

What are then the main causes for the improvement in efficiency using the water-rich mobile phases. For the monolithic polymers we previously proposed a model where slowly exchanging sites are made inaccessible due to water induced shrinkage of the material.[1] This explanation is supported by the significantly lower sample load capacity observed in the aqueous mobile phases.

**Frontal Analysis.** We anticipated that the higher surface area support (Si100: 380 $m^2/g$) would lead to materials useful for preparative applications. However, for Si100 materials with an average film thickness of 0.8 nm, this was not the case. Despite several attempts, the film thickness could not be increased further due to premature phase separation, presumably caused by the larger concentration of growing chains in solution. Instead, the wide pore silica (Si1000), with a film thickness of 3.8 nm, showed the highest saturation capacity. Figure 8 shows the isotherms obtained by frontal analysis using MIP6 in a water poor mobile phase. A pronounced difference in the adsorbed amount of the enantiomers is seen. From the differential isotherm, showing the excess binding of the L enantiomer, it is concluded that this difference exceeds previously determined saturation capacities of L-PA imprinted polymers.

**Comparison of Different Grafting Techniques.** The first comparison in this section concerns the covalent (MIP8, $d$ = 2.5 nm) vs noncovalent approach (MIP11, $d$ = 2.3 nm) to immobilize the azo initiator on a 30 nm pore size support material. Obviously, the noncovalent approach results in grafted films of poor quality, as seen in the much lower separation factor and resolution factor although some improvement is seen using the water-rich mobile phase (Figure 7C). However, in view of its simplicity and the fact that resolution was observed, further study of this approach is warranted.

We then compared the "grafting from" approach with materials prepared according to the "grafting to" approach previously described by Wulff et al.[18] The "grafting to" approach proved time-consuming and poorly reproducible. Photochemical grafting did not result in material showing enantioselectivity, whereas thermal polymerization for 24−48 h gave, in a few cases, materials exhibiting enantioselectivity. These materials did not offer any benefit over materials prepared according to the "grafting from" approach.

**Other Templates and Formats.** An interesting application of the materials would be to use them as supports in small scale combinatorial synthesis of MIPs.[33] For this purpose, it is necessary to demonstrate that the technique can be reproducibly applied to other templates and with smaller batches of material. Thus we used the triazine terbutylazine as template and performed the synthesis in triplicate using 50 mg of support material in 1.5 mL sample vials. After polymerization for 1 h, the materials were washed and subsequently reequilibrated with 1 mL of a solution of the template (0.1 mM in ACN). The MIPs bound 33% (±3%) while the corresponding nonimprinted polymers (NIPs) bound 13% (±%1) of the template. Interestingly these values are close to those obtained for correspond-

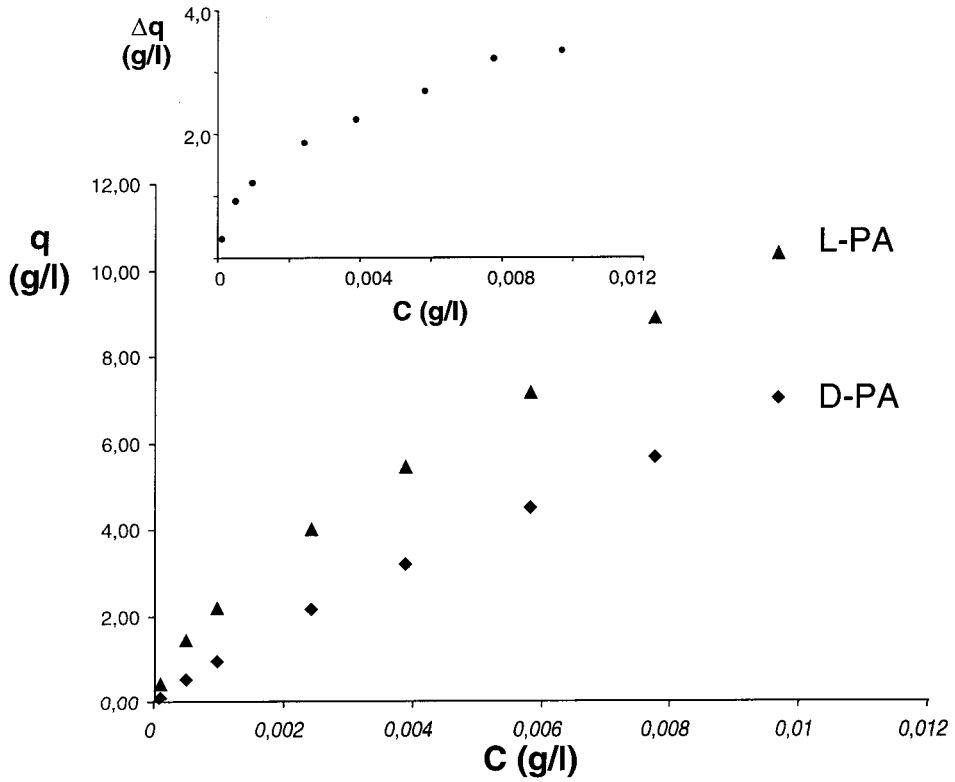


**Figure 8.** Isotherms of D- and L-PA determined by frontal analysis using a column packed with MIP6 and the mobile phase: ACN/AcOH/$H_2O$ 98.125/1.25/0.625 (v/v/v). The inset shows the corresponding plot of the excess binding of the L enantiomer.

ing monolith MIPs (containing a roughly 10× higher density of binding sites) in a 1 mM solution of the template. In this case, the MIPs bound ca. 38% and the NIPs ca. 15%. Thus the technique can be conveniently applied to other templates for a rapid production of beaded MIP composites.

## Conclusions

A new approach to prepare thin films of imprinted polymers on various support materials has been described. Since the morphology of the resulting composite materials is determined by the underlying support, this gives access to monodisperse, spherical imprinted particles with different pore sizes, particles sizes and to nonporous materials. Furthermore, this has the benefit of allowing the MIP films to be prepared using a variety of solvents and functional monomers, thus disregarding the effect of these parameters on polymer structure and morphology or the ability of these systems to yield stable suspensions. This allows the focus of the attention to be mainly on the search for conditions that result in high quality binding sites. The technique can be applied to different templates and exhibit distinct advantages over the conventional monolith procedure. Thus, the materials are obtained in a short time (1−2 h) and minimal work up is required. Assuming that the monomer solution can be recycled (Figure 2), the consumption of template can be significantly reduced.

Maybe even more important is the tunable film thickness, allowing materials to be optimized for either high efficiency analytical or high capacity preparative scale separations. Of particular interest is the high column efficiency ($N_D = 24000/m$) associated with the materials with the thinnest grafted films. This number compares favorably to many commercially available phases.

Finally, grafting of the polymers from nonporous materials gave rise to tightly packed agglomerates interconnected by an imprinted weblike polymer structure. The applications of this technique to prepare new, robust packings for capillary electrochromatography is presently under investigation.

**Acknowledgment.** We thank Gunnar Glasser (MPI für Polymerforschung, Mainz, Germany) for the SEM micrographs, Klaus Beckerle (Universität Mainz) for the DSC investigations, Milena Quaglia and Ersilia de Lorenzi (University of Pavia) for assistance with the frontal analysis and Dieter Lubda (Merck KGaA, Darmstadt, Germany) for the gifts of silica samples. Financial support from the Rheinland Pfalz Stiftung für Innovation is gratefully acknowledged.

**Supporting Information Available:** Text giving experimental details on synthesis and characterization and figures showing transmission IR spectra, mass loss curves and scanning electron micrographs. This material is available free of charge via the Internet at http://pubs.acs.org.

## References and Notes

(1) Sellergren, B., Ed. *Molecularly imprinted polymers. Man made mimics of antibodies and their applications in analytical chemistry*; Elsevier Publishers: Amsterdam, 2001; Vol. 23.
(2) Bartsch, R. A.; Maeda, M. *Molecular and Ionic Recognition with Imprinted Polymers*; Oxford University Press: Washington, DC, 1998.
(3) Wulff, G. *Angew. Chem., Int. Ed. Engl.* **1995**, *34*, 1812−32.
(4) Mosbach, K.; Ramström, O. *Bio/Technology* **1996**, *14*, 163−70.
(5) Sajonz, P.; Kele, M.; Zhong, G.; Sellergren, B.; Guiochon, G. *J. Chromatogr.* **1998**, *810*, 1−17.
(6) Shea, K. J.; Sasaki, D. Y. *J. Am. Chem. Soc.* **1991**, *113*, 4109−4120.

(7) Brunkan, N. M.; Gagne, M. R. *J. Am. Chem. Soc.* **2000**, *122*, 6217−6225.
(8) Haupt, K.; Mosbach, K. *Chem. Rev.* **2000**, *100*, 2495−2504.
(9) Andersson, L. I. *J. Chromatogr., B: Biomed. Sci. Appl.* **2000**, *745*, 3−13.
(10) Mayes, A. G.; Mosbach, K. *Anal. Chem.* **1996**, *68*, 3769−3774.
(11) Matsui, J.; Okada, M.; Tsuruoka, M.; Takeuchi, T. *Anal. Commun.* **1997**, *34*, 85−87.
(12) Strikovsky, A. G.; Kasper, D.; Gruen, M.; Green, H. J.; Wulff, G. *J. Am. Chem. Soc.* **2000**, *122*, 6295−6296.
(13) (a) Hosoya, K.; Yoshizako, K.; Tanaka, N.; Kimata, K.; Araki, T.; Haginaka, *J. Chem. Lett.* **1994**, 1437−8. (b) Haginaka, J.; Sanbe, H. *Anal. Chem.* **2000**, *72*, 5206−5210.
(14) Perez, N.; Whitcombe, M. J.; Vulfson, E. N. *J. Appl. Polym. Sci.* **2000**, *77*, 1851−1859.
(15) Sellergren, B. *J. Chromatogr. A* **1994**, *673*, 133−141.
(16) Lei, Y.; Cormack, P. A. G.; Mosbach, K. *Anal. Commun.* **1999**, *36*, 35−38.
(17) Ye, L.; Weiss, R.; Mosbach, K. *Macromolecules* **2000**, *33*, 8239−8245.
(18) Wulff, G.; Oberkobusch, D.; Minarik, M. *React. Polym., Ion Exch., Sorbents* **1985**, *3*, 261−275.
(19) Glad, M.; Reinholdsson, P.; Mosbach, K. *React. Polym.* **1995**, *25*, 47−54.
(20) Arnold, F. H.; Plunkett, S.; Dhal, P. K.; Vidyasankar, S. *Polym. Prepr.* **1995**, *36* (1), 97−8.
(21) Joshi, V. P.; Karode, S. K.; Kulkarni, M. G.; Mashelkar, R. A. *Chem. Eng. Sci.* **1998**, *53*, 2271−2284.
(22) Piletsky, S. A.; Matuschewski, H.; Schedler, U.; Wilpert, A.; Piletska, E. V.; Thiele, T. A.; Ulbricht, M. *Macromolecules* **2000**, *33*, 3092−3098.
(23) Schweitz, L.; Andersson, L. I.; Nilsson, S. *Anal. Chem.* **1997**, *69*, 1179−1183.
(24) (a) Brüggemann, O.; Freitag, R.; Whitcombe, M. J.; Vulfson, E. N. *J. Chromatogr.* **1997**, *781*, 43−53. (b) Tan, Z. J.; Remcho, V. T. *Electrophoresis* **1998**, *19*, 2055−2060.
(25) Lin, J.-M.; Nakagama, T.; Uchiyama, K.; Hobo, T. *J. Liq. Chromatogr. Relat. Technol.* **1997**, *20*, 1489−1506.
(26) Carlier, E.; Guyot, A.; Revillon, A. *React. Polym.* **1991/1992**, *16*, 115.
(27) Carlier, E.; Guyot, A.; Revillon, A. *React. Polym.* **1992**, *18*, 167.
(28) Prucker, O.; Rühe, J. *Macromolecules* **1998**, *31*, 602−613.
(29) Prucker, O.; Rühe, J. *Macromolecules* **1998**, *31*, 592−601.
(30) Quaglia, M.; De Lorenzi, E.; Sulitzky, C.; Massolini, G.; Sellergren, B. *Analyst* **2001**, *126*, 1495−1498.
(31) Lepistö, M.; Sellergren, B. *J. Org. Chem.* **1989**, *54*, 6010−6012.
(32) Tsubokawa, N.; Kogure, A.; Maruyama, K.; Sone, Y.; Shimomura, M. *Polym. J.* **1990**, *22*, 827−833.
(33) Lanza, F.; Sellergren, B. *Anal. Chem.* **1999**, *71*, 2092−2096.
(34) Guyot, A.; Hodge, P.; Sherrington, D. C.; Widdecke, H. *React. Polym.* **1991/1992**, *16*, 233−259.
(35) Verlaan, J. P. J.; Bootsma, J. P. C.; Challa, G. *J. Mol. Catal.* **1982**, *14*, 211−218.
(36) Dekking, H. G. G. *J. Appl. Polym. Sci.* **1965**, *9*, 1641−1651.
(37) Dekking, H. G. G. *J. Appl. Polym. Sci.* **1967**, *11*, 23−36.
(38) Velten, U.; Tossati, S.; Shelden, R. A.; Caseri, W. R.; Suter, U. W.; Hermann, R.; Müller, M. *Langmuir* **1999**, *15*, 6940−6945.
(39) Carlier, E.; Guyot, A.; Revillon, A.; Llauro-Darricades, M.-F.; Petiaud, R. *React. Polym.* **1991/1992**, *16*, 41−49.
(40) Tsubokawa, N.; Shirai, Y.; Tsuchida, H.; Handa, S. *J. Polym. Sci., A: Polym. Chem.* **1994**, *32*, 2327−2332.
(41) The choice of support is dictated by the required separation efficiency or sample load capacity of the materials.
(42) Unger, K. K. *Adsorbents in column liquid chromatography*; Unger, K. K., Ed.; Marcel Dekker Inc.: New York, 1990; Vol. 47, pp 331−470.
(43) The extent of one- vs two-point binding is not revealed by these methods but was estimated by Guyot et al. (see ref 39) based on solid state $^{13}C$ NMR data.
(44) Colthup, N. B.; Daly, L. H.; Wiberly, S. E. *Introduction to IR and Raman Spectroscopy*, 3rd ed.; Academic Press: New York, 1990.
(45) This distance is 5−6 Å assuming a syn conformation of the amidine groups and the trans configuration of the azo group.
(46) Moad, G.; Solomon, D. H. *The chemistry of free radical polymerization;* Elsevier Science Ltd.: Bath, England, 1995.
(47) Sherrington, D. C.; Hodge, P. *Synthesis and separations using functional polymers*; J. Wiley and Sons: Chichester, England, 1988.
(48) Sellergren, B.; Shea, K. J. *J. Chromatogr. A* **1995**, *690*, 29−39.
(49) Chen, Y.; Kele, M.; Sajonz, P.; Sellergren, B.; Guiochon, G. *Anal. Chem.* **1999**, *71*, 928−938.
(50) Sellergren, B.; Shea, K. J. *J. Chromatogr. A* **1993**, *635*, 31.
(51) Sellergren, B.; Shea, K. J. *J. Chromatogr. A* **1993**, *654*, 17−28.
(52) Sellergren, B.; Lepistö, M.; Mosbach, K. *J. Am. Chem. Soc.* **1988**, *110*, 5853−60.
(53) For grafting from surfaces using immobilised initiators it is particularly important to remove oxygen due to the small number of growing chains (see ref 28). Three freeze thaw cycles were therefore performed and the samples continuously purged with nitrogen during polymerization.
(54) Snyder, L. R.; Kirkland, J. J. *Introduction to Modern Liquid Chromatography*; Wiley: New York, 1979.
(55) Meyer, V. R. *Chromatographia* **1987**, *24*, 639.
(56) Miyabe, K.; Guiochon, G. *Biotechnol. Prog.* **2000**, *16*, 617−629.

MA011303W